DRL Line Item No. 10

DOE/JPL-954868-78/4
Distribution Category UC-63

AUTOMATED ARRAY ASSEMBLY, PHASE II

R. V. D'Aiello
RCA Laboratories
Princeton, New Jersey 08540

QUARTERLY REPORT NO. 4

OCTOBER 1978

This work was performed for the Jet Propulsion Laboratory, California Institute of Technology, under NASA Contract NAS7-100 for the Department of Energy.

The JPL Low-Cost Silicon Solar Array Project is funded by DOE and forms part of the DOE Photovoltaic Conversion Program to initiate a major effort toward the development of low-cost solar arrays.

Prepared Under Contract No. 954868 For

JET PROPULSION LABORATORY
CALIFORNIA INSTITUTE OF TECHNOLOGY
Pasadena, California 91103

DRL Line Item No. 10

DOE/JPL-954868-78/4
Distribution Category UC-63

AUTOMATED ARRAY ASSEMBLY, PHASE II

R. V. D'Aiello
RCA Laboratories
Princeton, New Jersey 08540

QUARTERLY REPORT NO. 4

OCTOBER 1978

This work was performed for the Jet Propulsion Laboratory, California Institute of Technology, under NASA Contract NAS7-100 for the Department of Energy.

The JPL Low-Cost Silicon Solar Array Project is funded by DOE and forms part of the DOE Photovoltaic Conversion Program to initiate a major effort toward the development of low-cost solar arrays.

Prepared Under Contract No. 954868 For

JET PROPULSION LABORATORY
CALIFORNIA INSTITUTE OF TECHNOLOGY
Pasadena, California 91103

PREFACE

This Quarterly Report, prepared by RCA Laboratories, Princeton, NJ 08540, describes the results of work performed from July 1, 1978 to September 30, 1978 in the Energy Systems Research Laboratory, B. F. Williams, Director; Materials and Process Laboratory, Solid State Division, Somerville, NJ, H. Veloric, Manager; and at the Advanced Technology Laboratory, Government and Commercial Systems, Camden, NJ, F. E. Shashoua, Director. The Project Scientist is R. V. D'Aiello and the Project Supervisor is D. Richman, Head, Semiconductor Materials Research. Others who participated in the research and writing of this report are:

J. Toner	-	cost analysis
D. Richman	-	silicon material
G. Schnable	-	metallization and AR coating
W. Kern	-	metallization and AR coating
K. Bube	-	metallization and AR coating
R. Scott	-	panel design and fabrication
P. Coyle	-	panel design and fabrication
E. Douglas	-	ion implantation
H. Veloric	-	manufacturing
L. Guarino	-	manufacturing

The JPL Task Manager is Don Bickler.

TABLE OF CONTENTS

LIST OF ILLUSTRATIONS

LIST OF ILLUSTRATIONS (Continued)

LIST OF TABLES

SECTION I

SUMMARY

During this quarter, progress was made in the following areas:

A. ION-IMPLANTED JUNCTION FORMATION AND SOLAR CELLS

A study was made of the performance of ion-implanted solar cells comparing the effect of two gettering techniques and three different starting silicon wafer materials. When the proper annealing or gettering treatment is applied, the results show little difference in cell performance within the categories of the starting silicon parameters chosen; however, the importance of obtaining long diffusion lengths is clearly illustrated. Solar cells having AM-1 efficiencies between 14 and 15% were consistently obtained when three-step furnace annealing was used.

Experiments were conducted to determine the optimum implant energy at a constant doping level. For the 5- to 100-keV energy range, the highest cell efficiencies were obtained at energies $\leq$15 keV.

B. SCREEN-PRINTED THICK-FILM METALLIZATION

Additional characterization of two RCA Ag metallization inks was performed. RCA n-type Ag containing 4.2 vol pct $AgPO_3$ was found to be marginally solderable when fired at 700 to 800°C for 10 min and unsolderable at higher concentrations and shorter firing times. Electrical conductivity tests indicated increasing conductivity with lower concentrations of $AgPO_3$ in the 8 to 30 vol pct range. Adhesion strength and failure mode results at 4.2 vol pct $AgPO_3$ are poor when fired at 800°C for 10 min. However, shorter firing times may improve solderability and adhesion.

The solderability of p-type metallization, containing 2.5 to 15 vol pct PBS frit ($80PbO-10B_2O_3-10SiO_2$ wt pct), has been characterized by contact angle measurements in the 600 to 900°C range for 1 to 10 min. Increasing solderability is noted with decreasing frit concentration, firing temperature, and time.

C. SPRAY-ON AR COATING

An alternative lower-cost second new source preparation based on titanium ethoxide has been developed for depositing low-cost antireflection (AR) coatings on metallized silicon solar cells by automated spraying. Effects of various component additives were studied, resulting in optimized and simplified solution compositions.

The post-deposition heat treatment sequence has been reduced to just 30 s each at 70°, 200°, and 400°C which will have a significant impact on increasing the production throughput capacity.

D. PANEL ASSEMBLY

Variations in the procedures for laminating the double-glass polyvinyl butyral (PVB) panel design were investigated. An initial procedure consisting of high vacuum, low laminating pressure, and a high softening temperature was found to allow considerable flow of the PVB and to result in successful laminations with reduced time in the autoclave.

SECTION II

INTRODUCTION

The purpose of our overall program is to establish technological readiness and provide verification for the elements of a manufacturing sequence which would ultimately be suitable for the large-scale production of silicon solar-array modules at a selling price of less than $500/kW. A program and process plan for accomplishing this objective was developed and put into operation during the first quarter. This plan is centered around the processing sequence shown in Fig. 1. Three junction-formation processes are shown; since our cost analysis shows that they do not differ greatly in cost, each should be considered for technical merits and possible future cost reduction. In Section III the progress made in the various process steps of the plan is described, and conclusions are presented in Section IV.

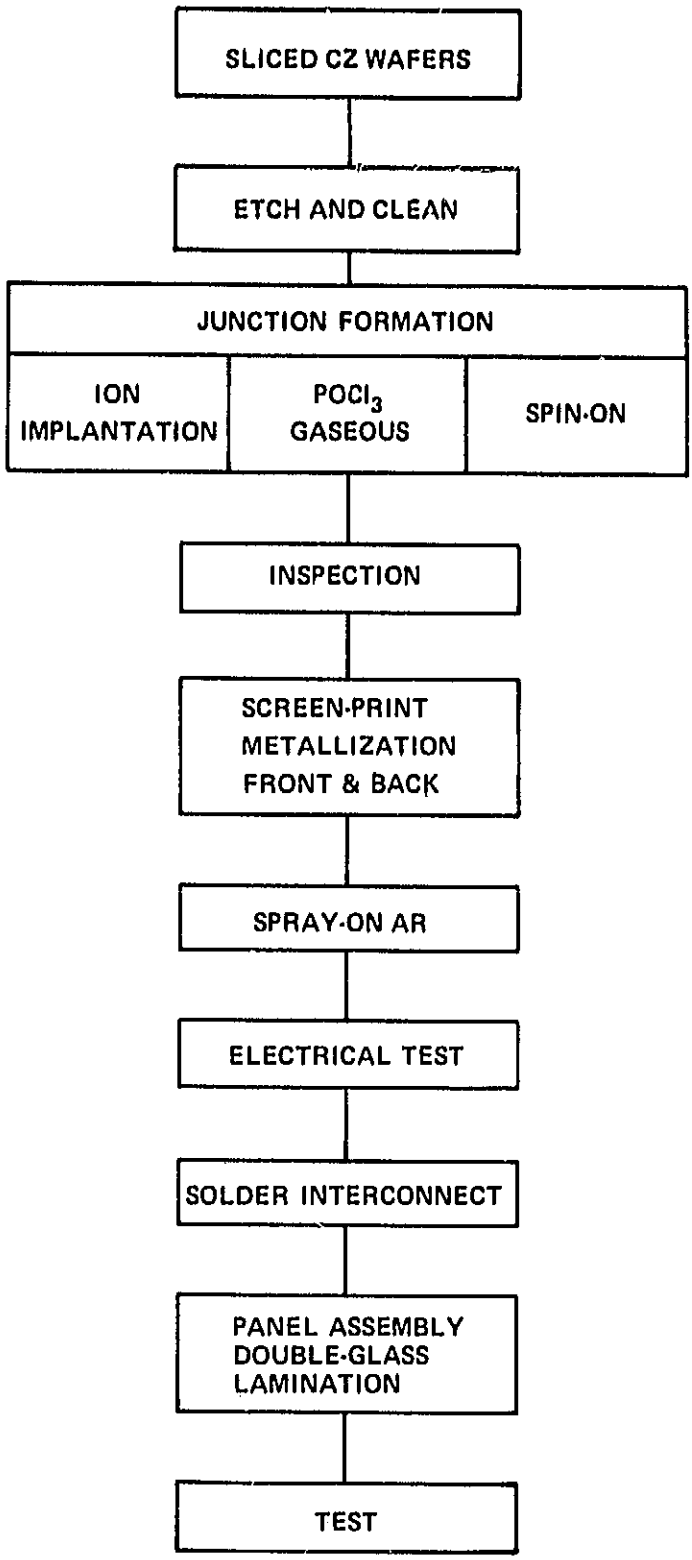

Figure 1. Major steps of process sequence.

SECTION III

PROGRESS

A. JUNCTION FORMATION - ION-IMPLANTED SOLAR CELLS

1. Furnace-Annealing Techniques

During this quarter, we have completed an experimental study of ion-implanted solar cells; the purpose of the study was to compare the effect of two gettering or annealing techniques and three different starting silicon wafer materials. The test conditions for this study are given in Table 1.

TABLE 1. ION-IMPLANTED SOLAR CELLS

1. Variables

Starting Silicon	Furnace Anneal Process
Monsanto* CZ 10-Ω-cm <100>	1. Boron-glass BSF (no back implant)
Monsanto CZ 1.5 Ω-cm <100>	2. Three-step anneal (^{11}B back)
Wacker** CZ 3 Ω-cm <100>	

2. Constants

Junction planar
Junction implant - ^{31}P, 4 x 10^{15} A/cm^2, 5 keV
Metallization - Ti/Ag evaporated (selected samples for screen printing)
AR coating - spin-on titaniumsilica film
Cell area - 4.5 cm^2

*Monsanto Co., St. Peters, MO.
**Wacker Chemical Corp., Richardson, TX.

All samples were implanted in a planar configuration on the junction side with ^{31}P at an energy of 5 keV and a dose of 4 x 10^{15} A/cm^2. Half the samples were designated for BSF gettering which consisted of the deposition of a boron glass on the back of the wafers followed by furnace annealing at 900°C for 30 min in nitrogen. The remaining wafers were subjected to a three-step anneal after a

boron implant (25 keV, 5 x 10^{15} A/cm^2) into the back, the anneal schedule consisting of 2 h at 500°C; 15 min at 850°C; and 2 h at 500°C. Seven solar cells and accompanying diagnostic diodes were fabricated in each category.

The average values and standard deviations for the AM-1 illuminated solar-cell parameters for all cells in the test are given in Table 2. Some observations concerning these results are:

(1) The samples treated with the three-step anneal showed uniformly excellent cell parameters. The maximum efficiency measured was 14.7%.

(2) The cells gettered with BSF boron-glass generally had lower efficiencies than those which received the three-step anneal.

(3) For the high-efficiency cells, there is little dependence on the starting silicon within the categories chosen.

(4) The variations of cell parameters as indicated by the standard deviations are small, indicating the uniformity and reproducibility of the ion-implantation process.

TABLE 2. ION-IMPLANTED MATRIX COMPARING GETTERING PROCESS AND STARTING WAFERS

Gettering Process	Starting Wafer	Silicon		$\bar{J}_{sc}$† (mA/cm^2)	σ_{sc} (mA/cm^2)	$\bar{V}_{oc}$ (mV)	σ_{oc} (mV)	$\overline{F.F.}$	$\sigma_{F.F.}$	$\bar{\eta}$†† (%)	σ_{η} (%)
Boron Glass BSF	M* 10 Ω-cm	<100>	CZ	28.8	0.61	529	7.7	0.769	0.005	11.7	0.3
Boron Glass BSF	M 1.5 Ω-cm	<100>	CZ	28.3	0.28	566	4.4	0.779	0.006	12.6	0.2
Boron Glass BSF	W** 3 Ω-cm	<100>	FZ	28.6	0.38	561	5.5	0.782	0.004	12.6	0.1
Three-Step Anneal	M 10 Ω-cm	<100>	CZ	32.0	0.52	580	5.5	0.764	0.024	14.2	0.5
Three-Step Anneal	M 1.5 Ω-cm	<100>	CZ	31.1	0.31	595	5.8	0.781	0.006	14.5	0.3
Three-Step Anneal	W 3 Ω-cm	<100>	FZ	31.0	0.30	590	4.9	0.785	0.008	14.3	0.3

*M = Monsanto
**W = Wacker
†Cell area = 4.5 cm^2
††AM-1 simulation ELH lamp at 100 mW/cm^2

The cells which received the three-step anneal exhibited excellent cell characteristics. The characteristics of one such cell measured in New Jersey sunlight on an exceptionally clear day are shown in Fig. 2. Under those conditions (17°C air ambient and an insolation of 101.9 mW/cm^2), the cell efficiency

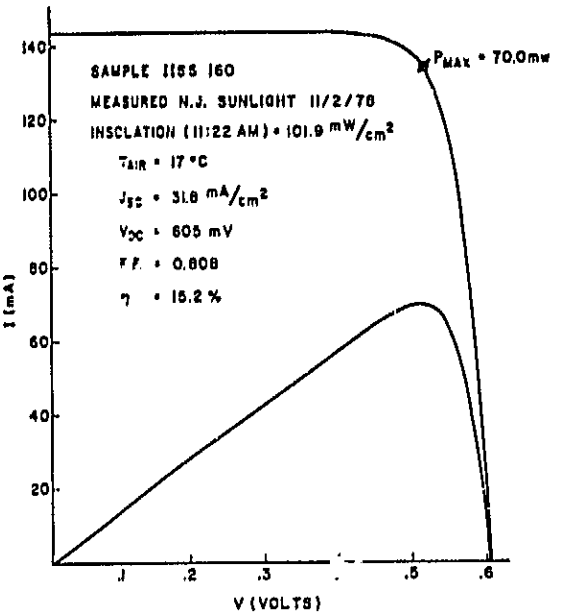

Figure 2. Power, I-V characteristics of an ion-implanted solar cell.

was 15.2%. That same cell measured at the standard temperature of 27°C under the ELH lamp simulator had an efficiency of 14.7%.

The lower efficiency results obtained with the boron-glass BSF cells are counter to our experience [1,2] with this gettering technique. On the basis of spectral response measurements and estimated diffusion lengths made for these samples, we suspect that the boron source or the anneal furnace has become contaminated. We are presently purchasing new BN wafers and replacing the furnace tube. It is interesting, however, to note the effect of diffusion length on the performance of these cells as compared with those annealed by the three-step process. Spectral responses and the cell parameters are given for two such cells in Fig. 3. It can be seen that the blue responses are equal but the peak and red responses are better for the cells annealed by the three-step process. The long diffusion length for the cells annealed by the three-step process also contributes to the higher values of open-circuit voltage.

1. R. V. D'Aiello, *Automated Array Assembly, Phase II,* Quarterly Report No. 3, prepared under Contract No. 954868 for Jet Propulsion Laboratory, June 1978.
2. R. V. D'Aiello, *Automated Array Assembly, Phase II,* Quarterly Report No. 2, prepared under Contract No. 954868 for Jet Propulsion Laboratory, March 1978.

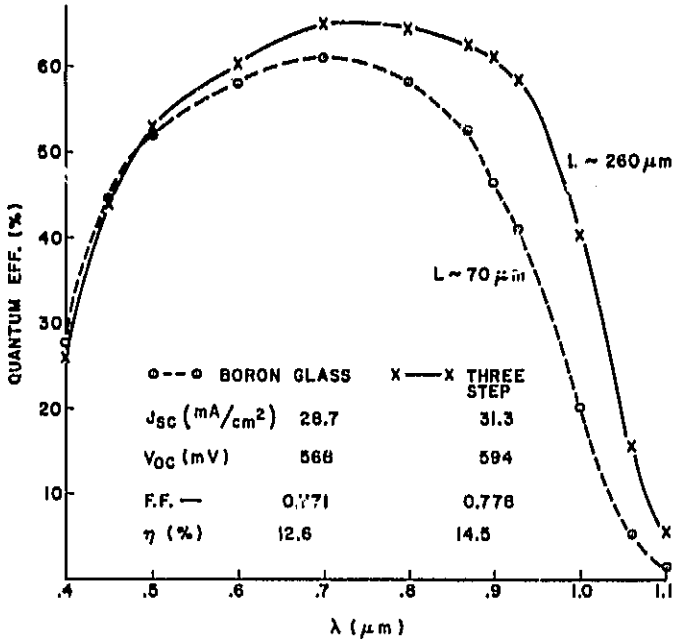

Figure 3. Comparison of spectra responses for ion-implanted cells with boron-glass BSF and three-step anneal.

2. Implant Energy

In the ion-implanted solar-cell studies conducted to date an implant energy of 5 keV was used under the assumption that low-implant energy causes less damage to the silicon surface layer and, after furnace annealing, results in a more desirable shallow impurity profile. In order to verify this idea, a series of cells was fabricated by implanting the ^{31}P at energies of 5, 15, 30, 50, 75, and 100 keV followed by a 900°C, 30 min, boron-glass (BSF) furnace anneal for all samples. The ^{31}P dose was adjusted at each energy to yield the same peak phosphorus concentration (5.65×10^{20} A cm^{-3}) in the surface layer.

The results of this experiment are shown in Figs. 4 and 5. From these data, it can be seen that the highest efficiency does occur for the low-implant energy due primarily to a fall-off in short-circuit current with increasing implant energy. This result could be due to one or more of several mechanisms associated with heavy doping effects combined with deep junctions or excess implant damage in the surface layer. Although the residual surface damage was not studied in these samples, the junction depths were measured, and the total phosphorus profiles were obtained by a secondary-ion mass spectroscopy (SIMS) analysis. These data, given in Figs. 6 and 7, show that quite deep junctions

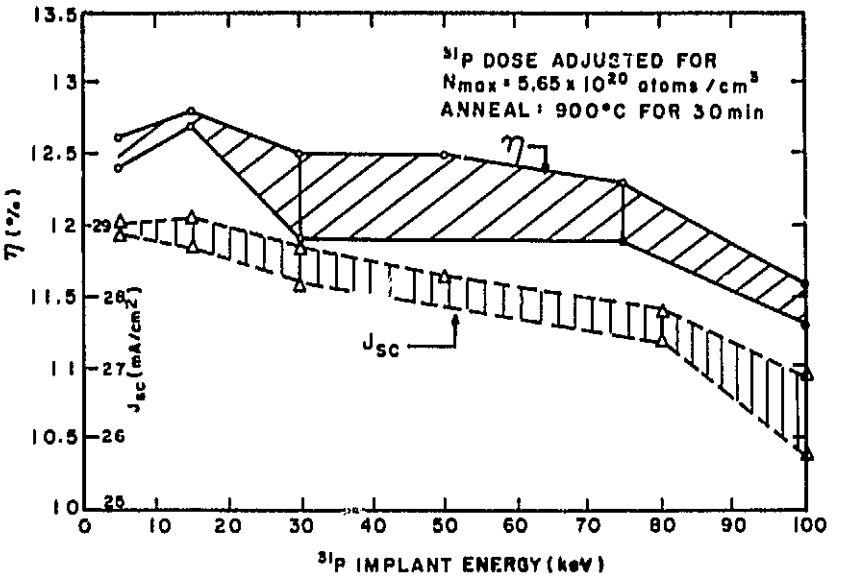

Figure 4. Efficiency and short-circuit current density as a function of implant energy.

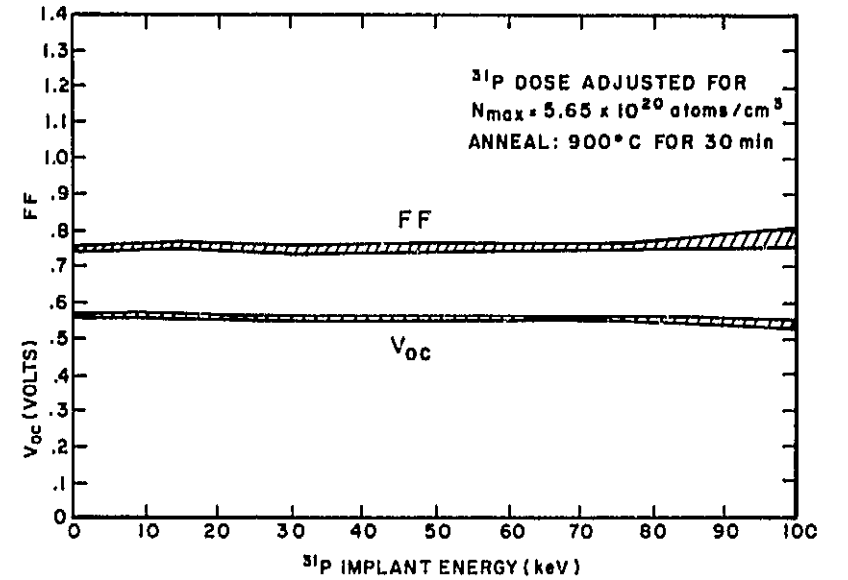

Figure 5. Fill-factor and open-circuit voltage as a function of implant energy.

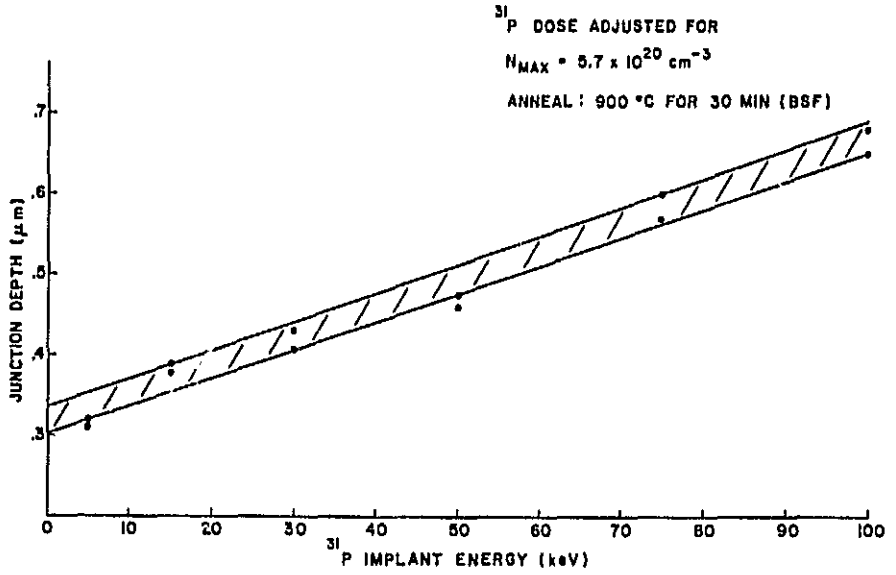

Figure 6. Junction depth as a function of implant energy.

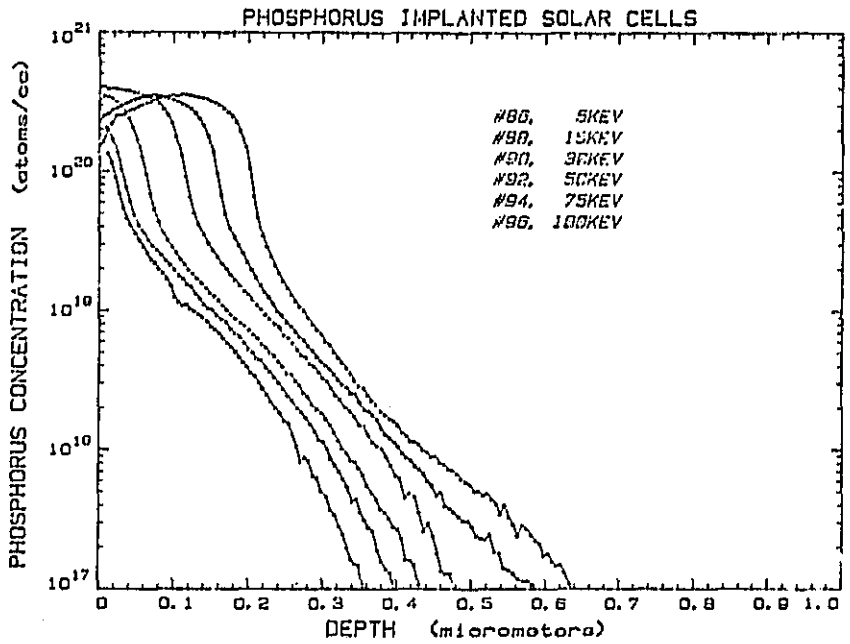

Figure 7. Phosphorus concentration profiles determined by SIMS for surface layers implanted at the energies shown in the inset. All samples annealed at 900°C for 30 min.

with heavily doped surface regions result from the implants at energies higher than 30 keV.

B. SCREEN-PRINTED METALLIZATION

1. n-Type Silver Metallization Ink

$AgPO_3$, precipitated with $AgNO_3$ and $NaPO_3$, was incorporated into a screenable ink containing Metz* FS type C flake silver, so that the final solids content was 80 wt pct. An 1874-square serpentine line (0.38 mm or 0.015 in. wide) was screen-printed onto 96% Al_2O_3 substrates, dried, and fired. Electrical and gravimetric measurements were made and the apparent percentage of bulk conductivity computed. Figures 8, 9, and 10 depict the changes in conductivity for firing times of 1, 2 and 5 min, respectively, at 600 to 900°C and $AgPO_3$ concentrations of 8.3 to 30.1 vol pct. If the three plots are superimposed, the conductivity results show the 5-min firing time to be slightly superior, but the 1- and 2-min firing times are almost identical. The similarity in conductivity results provides a wide latitude in processing time. Hence, optimization of metallization solderability and adhesion can proceed without too much concern for conductivity losses. The slight decline in conductivity between 8.3 and 30.1 vol pct $AgPO_3$ may imply that lower concentrations would provide higher conductivity. While apparently contrary to liquid-phase sintering theory, the extreme wettability, e.g., the 0° contact angle previously reported between Ag and $AgPO_3$, may account for very rapid sintering at lower concentrations than are usually observed.

A cursory examination of solderability of 4.2, 8.3, and 16 vol pct $AgPO_3$ inks showed the latter two to be unsolderable (with 62Sn-36Pb-2Ag wt pct and Kester** 1544 flux) when the inks were fired on Si at 800 or 900°C for 1 or 2 min. The 4.2 vol pct-$AgPO_3$ ink produced contact angles of 90 to 95° when the ink was fired at 700 or 800°C for 10 min. Adhesion strengths, however, were lower than the p-type (PBS frit-based) ink with failure frequently occurring at the Cu strap-metallization interface.

*Metz Metallurgical Co., South Plainfield, NJ.
**Kester Solder Co., Chicago, IL.

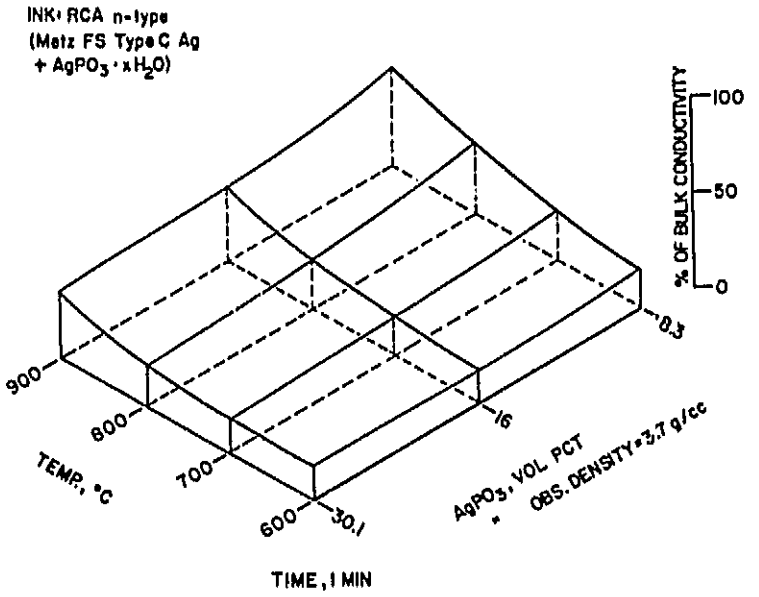

Figure 8. Conductivity versus temperature and vol pct $AgPO_3$ for RCA n-type ink. Firing time = 1 min.

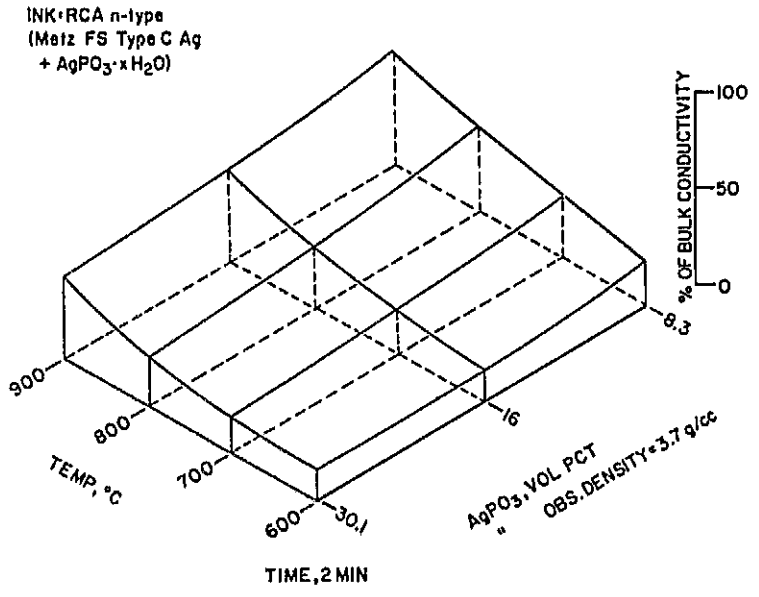

Figure 9. Conductivity versus temperature and vol pct $AgPO_3$ for RCA n-type ink. Firing time = 2 min.

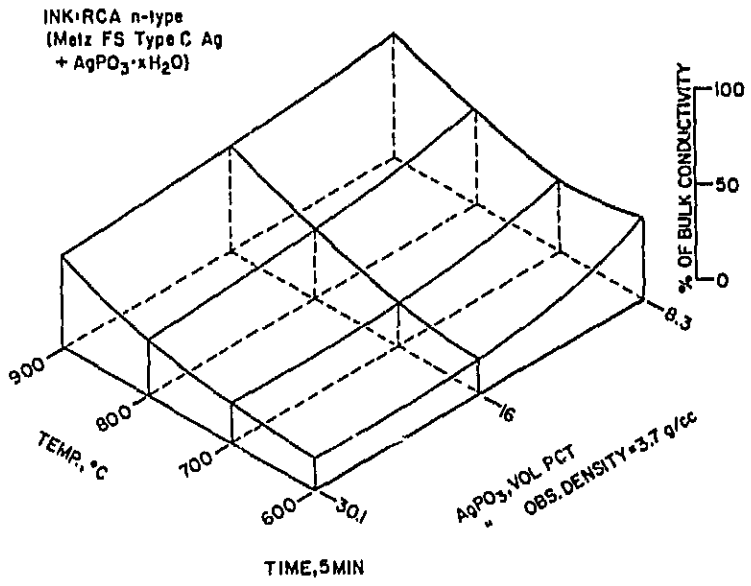

Figure 10. Conductivity versus temperature and vol pct $AgPO_3$ for RCA n-type ink. Firing time = 5 min.

2. p-Type Silver Metallization Ink

Inks containing 2.5, 5.0, and 15 vol pct PBS ($80PbO-10B_2O_3-10SiO_2$ wt pct) frit and Metz FS Type C flake silver were formulated in a manner similar to the n-type inks. Samples for solderability contact angle measurements on n- and p-type Si were prepared by screen printing, drying, and firing at 600 to 900°C for 1 to 10 min for the p-Si and 700 to 800°C for 1 to 2 min for the n-Si substrates. Solder balls composed of 62Sn-36Pb-2Ag were reflowed at 215°C for about 5 s in the presence of Kester 1544 flux. After flux removal, contact angle measurements were taken, and Figs. 11, 12, and 13 illustrate the results for the p-Si substrate bearing 2.5, 5.0, and 15 vol pct PBS frit-based metallizations, respectively. In each ink it is clear that solderability improves with decreasing firing time and temperature as shown by the decreasing contact angles. If the curves are superimposed, solderability is also seen to improve with decreasing frit content, as expected.

In Figs. 14, 15, and 16 contact angles on n-Si are shown for the 2.5, 5.0, and 15 vol pct PBS frit-based inks, respectively, for the limited temperature and time range of interest, e.g., 700 to 800°C for 1 to 2 min. Compared with the p-Si substrate, the results on the n-Si substrate are almost identical.

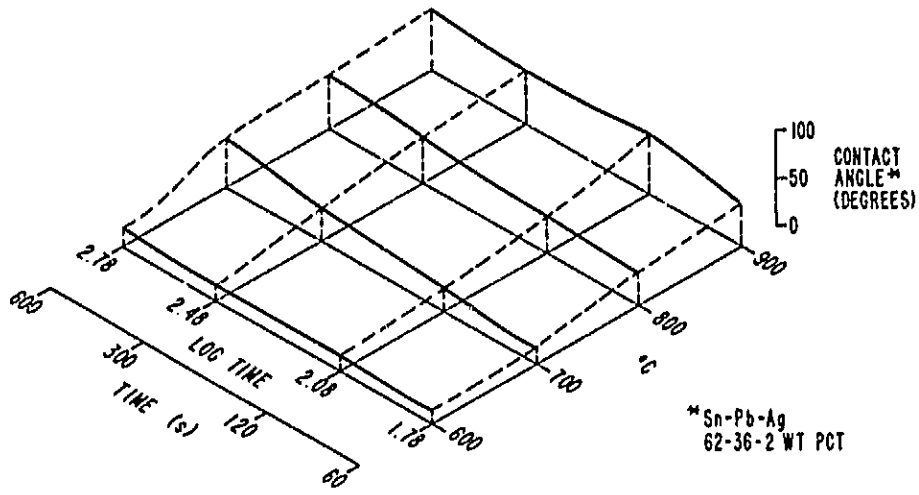

Ag (METZ FS TYPE C)+2.5 VOL PCT PBS FRIT ON p-SI

Figure 11. Wet solder contact angle as a function of firing temperature and time for Ag + 2.5 vol pct PBS ink on p-silicon.

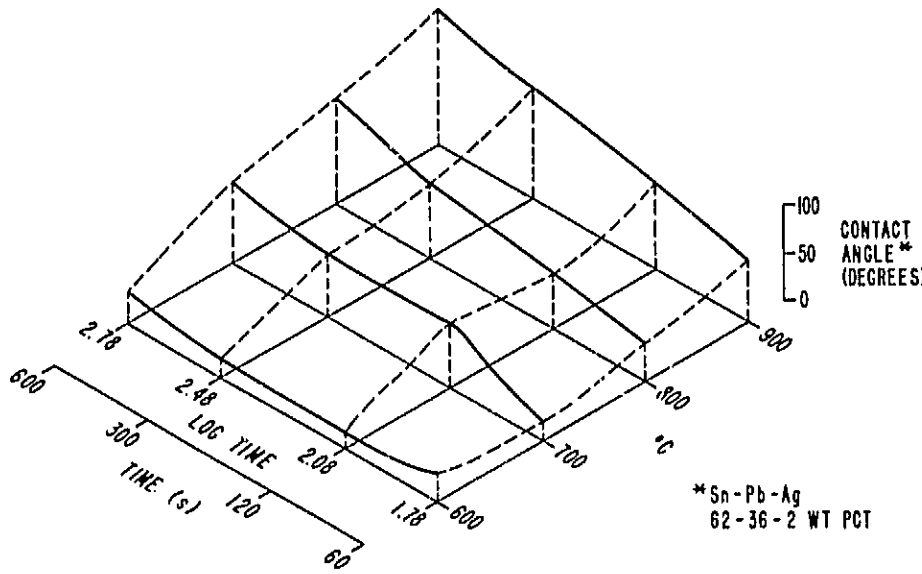

Ag (METZ FS TYPE C)+5 VOL PCT PBS FRIT ON p-SI

Figure 12. Wet solder contact angle as a function of firing temperature and time for Ag + 5 vol pct PBS ink on p-silicon.

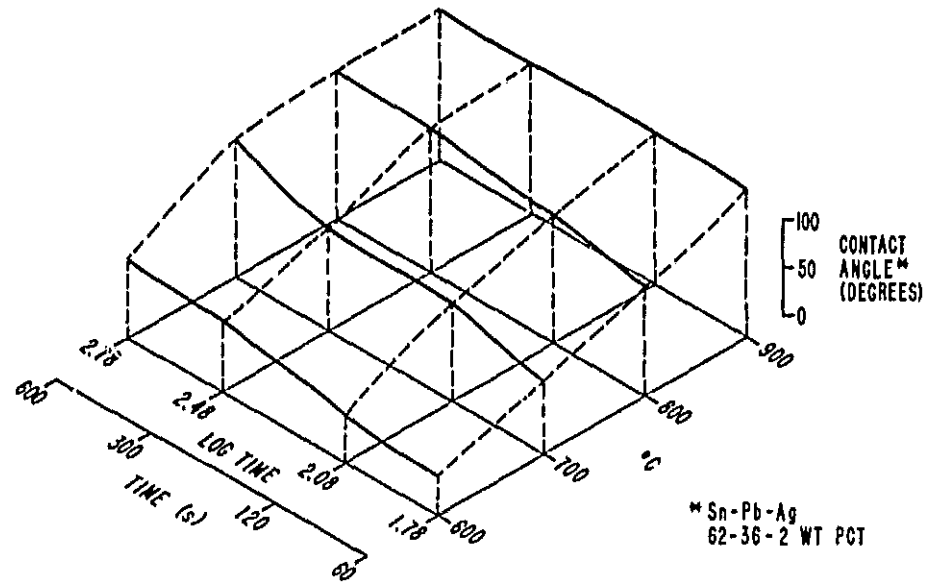

Ag (METZ FS TYPE C) +15 VOL PCT PBS FRIT ON p-SI

Figure 13. Wet solder contact angle as a function of firing temperature and time for Ag + 15 vol pct PBS ink on p-silicon.

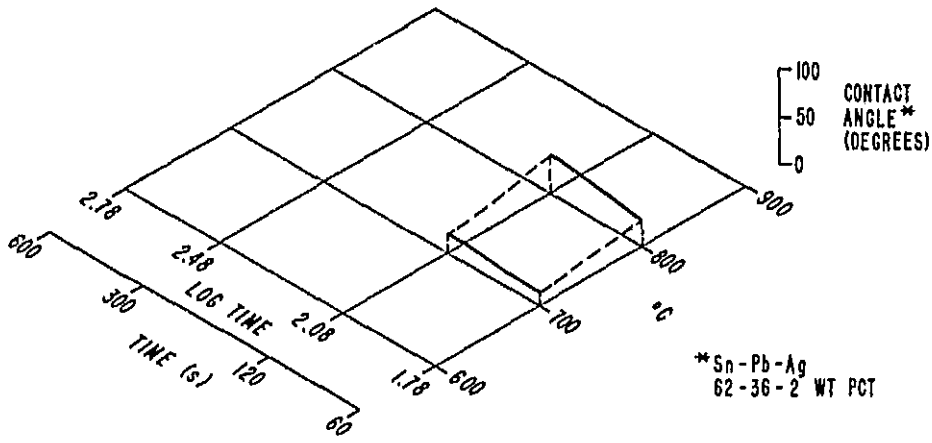

Ag (METZ FS TYPE C) +2.5 VOL PCT PBS FRIT ON n-SI

Figure 14. Wet solder contact angle as a function of firing temperature and time for Ag + 2.5 vol pct PBS ink on n-silicon.

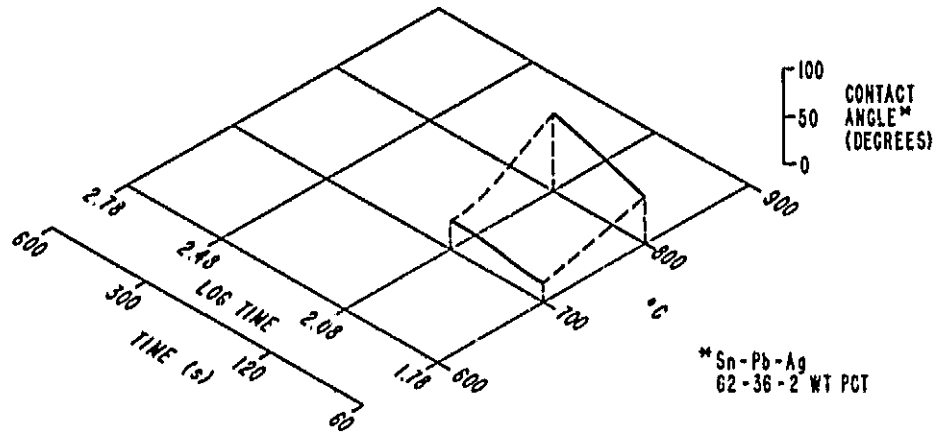

Ag (METZ FS TYPE C)+5 VOL PCT PBS FRIT ON n-Si

Figure 15. Wet solder contact angle as a function of firing temperature and time for Ag + 5 vol pct PBS ink on n-silicon.

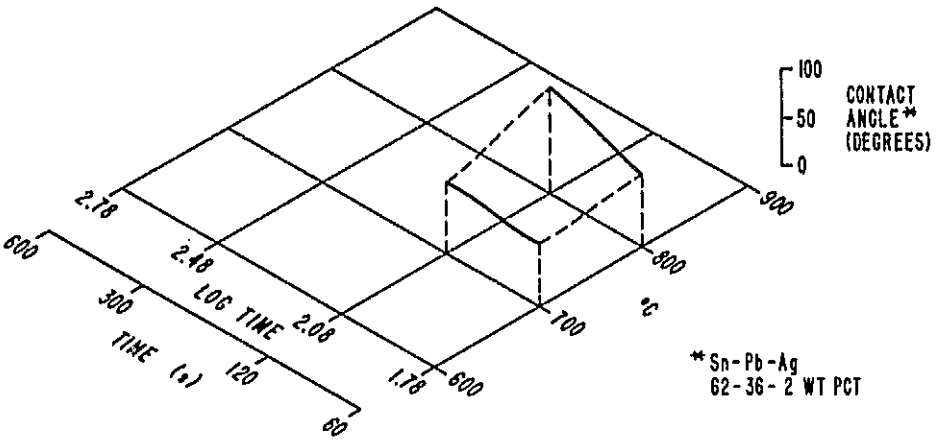

Ag (METZ FS TYPE C)+15 VOL PCT PBS FRIT ON n-Si

Figure 16. Wet solder contact angle as a function of firing temperature and time for Ag + 15 vol pct PBS ink on n-silicon.

Therefore, in terms of solderability and conductivity (previously reported) p-type (PBS frit) ink would serve as an adequate alternative to n-type ($AgPO_3$) ink.

C. 'SPRAY-ON ANTIREFLECTION COATINGS

1. New Source Solutions for AR Coatings

In Quarterly Report No. 3 [1] we briefly reported on the formulation of our own source solution based on titanium isopropoxide for depositing AR coatings on metallized silicon solar cells with better materials control and at substantially reduced materials cost.

During the present reporting period we have introduced, as an additional alternative, a second new source solution based on titanium ethoxide, studied the effects of diluents and modifying agents at various mixing ratios, and formulated simplified optimum solution compositions for the two systems. The effectiveness of the AR coatings from these source solutions has been demonstrated by comparative electrical measurements of cell performance and found to be at least as good as those obtained from the commercial source solution.

The physical and chemical requirements of a sprayable solution for producing AR coatings were discussed in Quarterly Reports Nos. 2 [2] and 3 [1]. The composition of our source solutions and the function of each component can be summarized as follows: (1) organometallic titanium compound as the essential primary reactant, (2) a miscible ester diluent solvent, (3) a lower aliphatic alcohol as a film leveling agent, and (4) 2-ethyl-1-hexanol as the key component for rendering the solution successfully sprayable.

Suitable organometallic titanium reactants include soluble titanium compounds which are hydrolyzable and can be readily oxidized and stabilized at temperatures at or below 400°C to form adherent and uniform titanium oxide films which have a refractive index of n = 2.0 to 2.2. The titanium compounds we prefer and have demonstrated to perform excellently are titanium alkoxide compounds such as titanium isopropoxide and titanium ethoxide.

The titanium compound is dissolved or diluted initially with an inert diluent such as butyl acetate, ethyl acetate and the like to form a one-phase solution. Suitably, the titanium compound is admixed in a ratio of 1:2 to 1:4 by volume, preferably 1:3 by volume, with the ester diluent.

Certain organometallic silicon compounds can be added at appropriate ratios if refractive index values of less than 2.0 are required. However, for our purpose of AR coating solar cells no such addition is necessary.

A key ingredient that renders the solution suitable for automated spray processing with the required stringent quality control of the film is 2-ethyl-1-hexanol. The physical characteristics of this compound appear to be unique in that when admixed with the other composition ingredients, it has the ability to effect spreading of the solution evenly across the substrate; this is due to the compound's surface tension and viscosity characteristics which promote wetting and improve the uniformity of the film. The compound has an appropriate vapor pressure causing it to evaporate slowly enough that the liquid film is not disrupted during the evaporation. Therefore, a uniform film can be applied to the substrate and dried to form a uniform continuous film of a titanium compound on the substrate.

Of the lower aliphatic alcohols to serve as leveling agent, we found isopropanol particularly effective. The sprayed-on solution mixture without an aliphatic alcohol thickens up along the metallization grid lines. The effect can be reversed by adding isopropanol, resulting in thinning along the metallization grid lines if an excessive quantity is added. A carefully balanced ratio can effect leveling of the liquid film along the metallization grid lines, resulting in a solid AR film of partically uniform thickness throughout the surface of the solar-cell areas between grid lines.

The spray solution ingredients are mixed in such proportions that the resultant solution can be applied evenly using spray techniques to form a liquid film of a desired thickness. The exact proportions can be varied within some limits, although the 2-ethyl-1-hexanol should be present in at least about 33% by volume of the spray solution. Not more than a maximum of about 33% by volume of the lower aliphatic alcohol should be present; the exact ratio depends on the thickness and morphology of the metallization system and must be optimized by empirical tests.

Numerous compositional ratios for both titanium compounds have been prepared and examined by automated spraying on test substrates and on solar-cell wafers. We found the optimal and simplified compositional ratios by volume for the spraying solution to be in the following range:

Titanium isopropoxide or Titanium ethoxide	1 vol	8.3 vol %
Butyl acetate	∿ 3	∿ 25
2-Ethyl-1-hexanol	≥ 4	≥ 33.3
Isopropanol	≤ 4	≤ 33.3
Total	∿12 vol	∿100 vol %

2. Effectiveness of AR Coating Source Solutions

The effectiveness of AR films produced from the two optimized spray source solutions, "RCA I" and "RCA II," were assessed by automatic spraying with a Zicon* autocoater. A source solution we prepared from Emulsiton** Titaniasilica "C" concentrate was also tested under identical conditions for comparison. A set of 3-in.-diameter silicon solar cells with etched surfaces and screen-printed Ag-metallization grids were used as the test substrate for each solution. The cells were of only mediocre electrical quality, and were spray-processed without special prior cleaning to examine the worst-case situation. Measurements of film thickness across the wafers were carried out by ellipsometry after heat treating the films step-wise at 70°, 200°, and 400°C for only 30 s each. Electrical efficiency evaluation by standard I_{sc} and V_{oc} measurements of the cells before and after coating with the AR films showed the RCA preparations to be at least as good as the commercial source solution. A summary of the results is presented in Table 3. It is important to point out that the greatly reduced heat-treatment times appear to be adequate for producing stable AR films. The practical consequence of the finding means a substantially increased production throughput capacity. More detailed tests and film analyses concerning this significant factor are being completed.

3. Effectiveness of AR Films as a Function of Thickness

The quality and performance of the AR films from any of the three source solutions can be expected to be constant if all materials, cell surfaces,

*Zicon Corp., Mount Vernon, NY.
**Emulsitone Co., Whippany, NJ.

TABLE 3. EFFECTIVENESS OF AR FILMS FROM THREE SOURCE SOLUTIONS

Source Solution	Vol. Ratio	Vol. %	Film Thickness (Å)	Performance Effectiveness* I_{sc} AR coated/I_{sc} uncoated	Increase %
Emulsitone					
Titaniasilica "C" concentrate	1	33.3			
Butylacetate	0	0			
2-ethyl-1-hexanol	1	33.3	833	1.32	32
Isopropanol	1	33.3			
RCA I					
Titanium isopropoxide	1	8.3			
Butyl acetate	3	25.0	824	1.35	35
2-ethyl-1-hexanol	4	33.3			
Isopropanol	4	33.3			
RCA II					
Titanium ethoxide	1	8.3			
Butyl acetate	3	25.0			
2-ethyl-1-hexanol	4	33.3	848	1.36	36
Isopropanol	4	33.3			

*These ratios indicate the increase in short-circuit current of the cells after AR coating; they can be considered essentially equivalent of the increase in efficiency, since V_{oc} remains unchanged after coating.

metallization, and spray processing conditions are well controlled and kept fixed. However, minor fluctuations in the spray processing could easily affect the film thickness. It is therefore imperative to ascertain experimentally the effect of film thickness on the performance of the AR coatings. All three source solutions (Emulsitone C, RCA I, RCA II) were tested by using them for coating typical 3-in.-diameter solar cells with screen-printed Ag-metallization patterns. Film thicknesses of nominally 600, 660, 730, and 800 Å (after heat treatments) were examined. Film deposition in this experimental matrix was done by centrifuging, mainly because intended variations in film thickness are more easily attained than by spraying. A second reason was to demonstrate that the effectiveness of the AR coatings is essentially independent of the method of film deposition and is solely a function of the optical film properties. Measurements of the coating efficiency were done as described in the preceding section. The compositions of the source solutions especially made for these spinning applications are listed in Table 4.

TABLE 4. COMPOSITION OF SOURCE SOLUTIONS FOR SPINNING APPLICATIONS

Nominal Film Thickness (Å)	Emulsitone C (vol)	Butyl Acetate (vol)	Spin Speed (r/min)	Ti-Propoxide (vol)	Butyl Acetate (vol)	Spin Speed (r/min)	Ti-ethoxide (vol)	Butyl Acetate (vol)	Spin Speed (r/min)
800	1	0	4500	1	3	7500	1	5	3500
730	1	0	6000	5	22	5500	1	5	4000
660	1	0	7200	5	22	4000	1	5	4900
600	6	1	6200	5	22	3500	1	5	6500

A summary of essential data and results from the solar-cell efficiency evaluation is presented in Table 5. Four major conclusions can be drawn:

(1) The AR efficiency of the three types of coatings is essentially unaffected by the film thickness in the range studied (600 to 800 Å); slight variations in film thickness are therefore not as as critical as had been assumed previously on the basis of quarter-wavelength optical theory.

TABLE 5. INCREASE IN CELL EFFICIENCY AS A FUNCTION OF AR FILM THICKNESS FOR THREE SOURCE SOLUTIONS

Nominal Film Thickness (Å)	Thickness ($Å_p$)*	Emulsitone C			RCA I (titanium isopropoxide-based)			RCA II (titanium ethoxide-based)		
		Thickness ($Å_e$)**	Refractive Index (n)	Increase† (%)	Thickness ($Å_e$)**	Refractive Index (n)	Increase† (%)	Thickness ($Å_e$)**	Refractive Index (n)	Increase† (%)
800	810	803	2.043	34	742	2.177	31	750	2.186	31
730	740	734	2.026	31	680	2.181	38	687	2.189	36
660	650	684	2.018	28	632	2.181	35	626	2.183	37
600	600	609	2.012	33	545	2.193	35	550	2.189	34
Average			2.025	32		2.183	35		2.187	36

*$Å_p$ = Thickness measurements by profilometry (Tencor stylus instrument).

**$Å_e$ = Thickness measurements by ellipsometry using green Hg light of 5461-Å wavelength.

† Increase determined by measuring short-circuit currents I_{sc} after/before coating.

(2) The average increase in cell efficiency after coating is 32% for the Emulsitone C film, 35% for the RCA I (titanium isopropoxide derived) film, and 36% for the RCA II (titanium ethoxide derived) film.

(3) Films deposited by centrifuge spinning exhibit similar efficiency increases as those deposited by automated spraying (Table 3), both ranging from 31 to 36% in the 800- to 850-Å wavelength region.

(4) The maximum efficiency increase for the three source solutions is 34% at 800 Å for Emulsitone C, 38% at 680 Å for RCA I, and 37% at 630 Å for RCA II.

The AR films created from the RCA source solutions are thus superior in effectiveness to those derived from the commercial source solution, and, as previously pointed out, can be obtained at a very substantial materials cost reduction.

D. INTERCONNECT AND PANEL ASSEMBLY

1. PVB Lamination

Two attempts were made to produce a full 4-ft^2 panel which could be subjected to the 50 lb/ft^2 cyclic wind loading test. Both panels were broken due to handling accident and/or improper cool-down procedures by the laminator (Figs. 17 and 18). In order to achieve the desired 4-ft^2 panel dimension, a border (unfilled with cells) was included due to unavailability of optimum diameter cells. In the first lamination (Fig. 17) complete PVB flow was not achieved due to premature edge-seal formation which trapped air inside the panel. The second panel (Fig. 18) laminated perfectly with all areas completely void free. Several cells cracked due to solder lumps remaining from hand-soldering operations. This problem will be alleviated with the radiant-heat mass-soldering technique.

We investigated a modification of the laminator's standard production process to determine if we could reduce the possibility of cell fracture and also reduce the duration of the autoclaving process. The duration of the autoclaving is proportional to the amount (mass) of air remaining after the initial flow of the PVB. The laminator's standard process consists of drawing

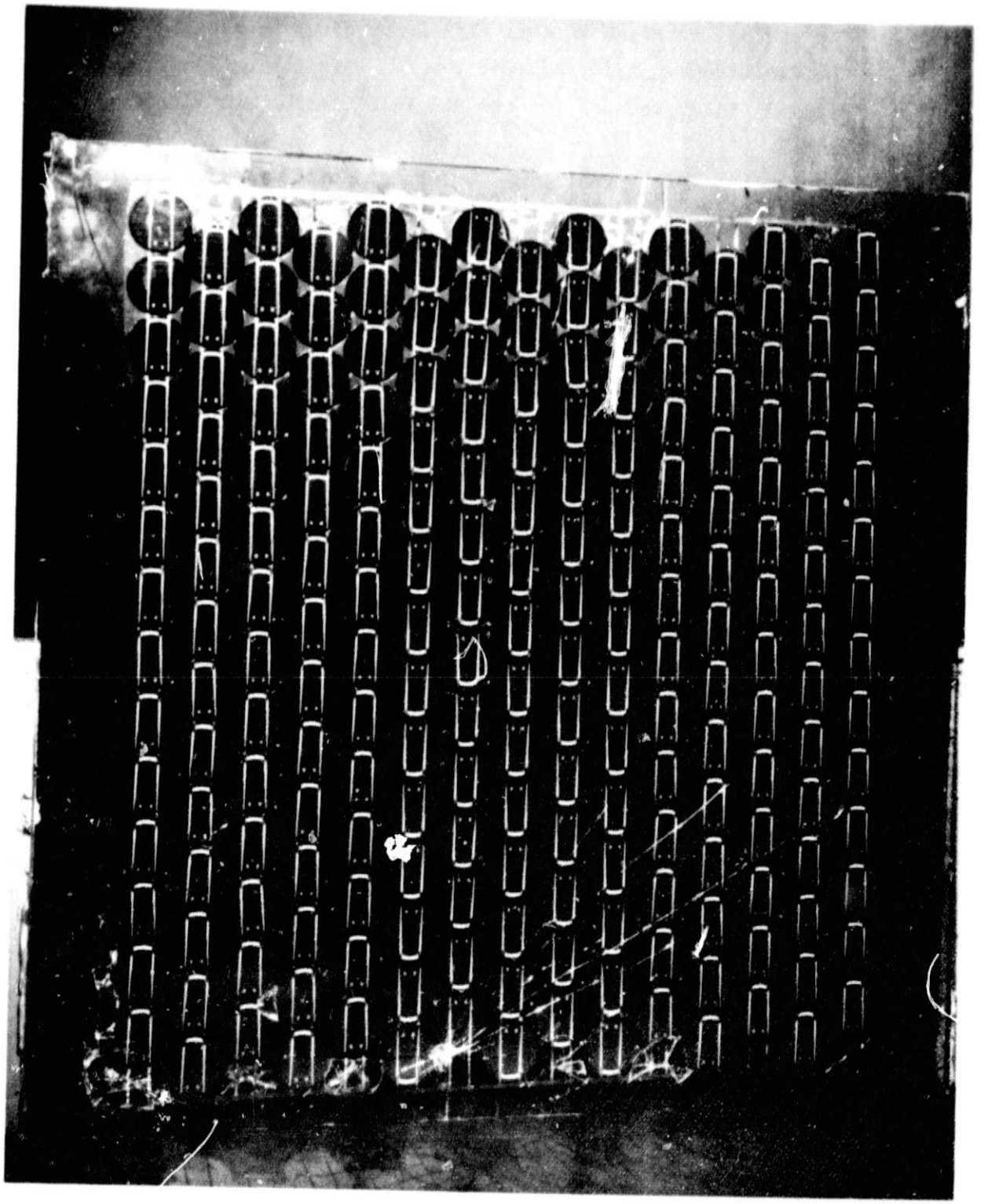

Figure 17. Front view of first 4-ft^2 panel. Premature edge seal caused trapped air inside panel. Starburst fracture at lower center of panel (both sides) may be due to thermal strain.

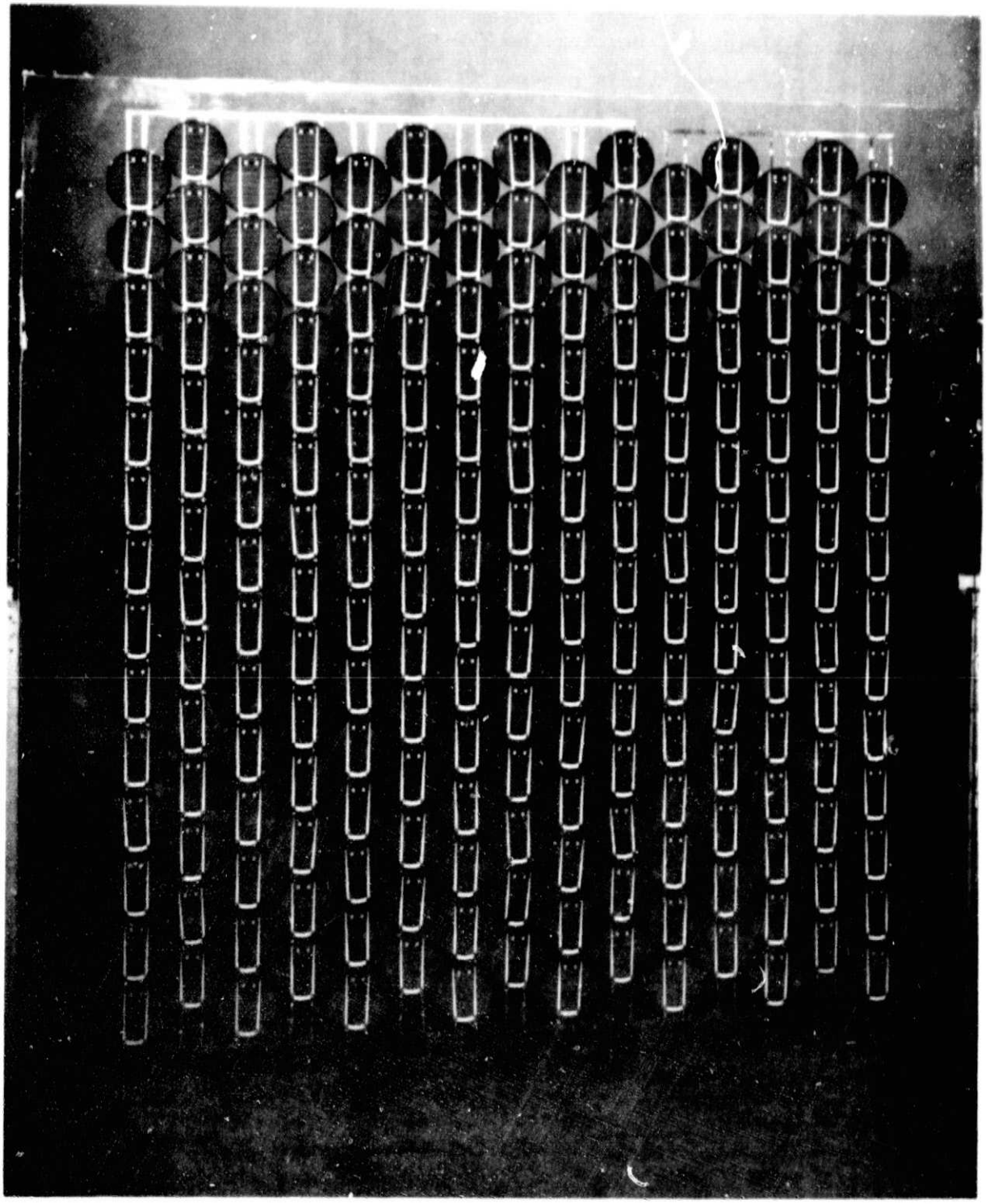

RCA PC-781149-C

Figure 18. Front view of second 4-ft^2 panel. This panel has no voids. Starburst cracks are believed due to presence of foreign matter between the glass and glass pressure plates used to preserve flatness during autoclaving.